Theoretical bcc ⇆ fcc Transitions in Metals via Bifurcations under Uniaxial Load

Frederick Milstein, Jochen Marschall,* and Huei Eliot Fang†
Departments of Materials and Mechanical Engineering, University of California, Santa Barbara, California 93106-5070
(Received 26 August 1994)

Pseudopotential models are used to study large strain, axial loading of the alkali metals. Various bcc ⇄ fcc transitions are found to be associated with bifurcations from primary to secondary branch paths, under strict uniaxial load. Theoretically, other systems (e.g., the β-brasses) are expected to behave similarly.

PACS numbers: 62.20.Dc, 61.50.Ks, 64.70.Kb, 81.40.Jj

In recent years, interest in homogeneous, large strain, nonhydrostatic deformation of crystal lattices has accelerated; see, e.g., Refs. [1–3] and the citations therein. Here we examine theoretical bcc → fcc transitions in the alkali metals under uniaxial stresses in the framework of a pseudopotential model. Three modes of deformation under uniaxial loading are studied: one follows a Bain deformation on a "primary" path of [100] loading (i.e., the crystal structure remains tetragonal), the other two branch (or bifurcate) from the primary tetragonal path to a secondary path of body centered (bc) or face centered (fc) orthorhombic crystal symmetry. This work is important theoretically because it (a) is apparently the first in which quantum mechanically based crystal models are used to study the bcc → fcc transitions associated with bifurcations among *uniaxial* loading paths of different crystallographic symmetry, (b) displays a thorough analogy in behaviors of the distinct branch paths and associated phase transitions, (c) points up the special role of a stress-free tetragonal state that occurs on each path, coincident with a local internal energy maximum, and (d) indicates that the magnitudes of the uniaxial compressive and tensile stresses required to initiate the bcc → fcc transitions in K, Rb, and Cs are about 2 orders of magnitude less than the "hydrostatic" pressures at which the transitions are observed. These results thus suggest that the combined effect of a relatively small uniaxial component of stress "superimposed" on a large hydrostatic compression could cause a bcc → fcc transition well before it would occur in the absence of the uniaxial component. This is an important consideration for high pressure experimentation, particularly since the alkali metals, K, Rb, and Cs exhibit bcc → fcc transitions under pressures P ranging from about 2 (for Cs) to 11 GPa (for K) [4], whereas some computations have suggested corresponding theoretical transformation pressures as high as about 50 GPa for K and Rb [4] [the computational model used in the present study exhibits the respective transitions (for K and Rb) at 37.0 and 25.8 GPa]. In addition, Na and Li undergo low temperature, atmospheric pressure, transitions from bcc to close packed structures that resemble fcc with periodic stacking faults [4]. Our results suggest experimentally verifiable effects of variously oriented *uniaxial* stresses on these low temperature transitions.

Branching of a crystal structure under uniaxial load was first observed computationally by Milstein and Huang [5], who studied the large strain elastic behavior of a Morse model of an fcc Ni crystal. They computed the path describing the mechanical response of the crystal as it was deformed uniformly under a [110] uniaxial load and found this path to branch from the path describing uniform deformation of the (initially) bcc configuration of the crystal under [100] uniaxial loading. The branching occurred under "dead" load [6] at a point coincident with the mutual equality of the (strain dependent) elastic moduli C_{22} and C_{23} [7]. The branch point, however, was found to be embedded in an elastically unstable region of deformation space (as was the unstressed bcc state). Milstein and Farber [8] used similar lattice model computations to study the analogous, but distinct, branching in which the path, corresponding to the [110] uniaxial loading of an (initially) bcc crystal, branched from the path of [100] loading of an (initially) fcc crystal. There the branch point was found to terminate an elastically stable region of the [100] loading path, in tension. Milstein and Farber [8] used theoretical arguments, supported by these computations, to show that, for a fcc crystal homogeneously deformed under a strict [100] uniaxial tensile load, a path of minimum energy takes the crystal into an unstressed bcc configuration, via the bifurcation that occurs at $C_{22} = C_{23}$. The fcc → bcc transition under uniaxial tension was also observed by Wang *et al.* [2] in a recent molecular dynamics study of an embedded atom model of fcc Au.

The present crystal mechanics computations employ the Heine-Abarenkov local model potential and the Taylor approximation for electron correlation and exchange in the dielectric function. With but two empirical parameters (which were determined for each of the alkali metals in Ref. [9]), the model was shown [9,10] to give good descriptions (when compared with experiment) of numerous properties, including the pressure-versus-volume behavior, the bcc → fcc transformations under pressure, and, at low temperature and atmospheric pressure, the bind-

 © 1995 The American Physical Society

ing energy E_{bind}, the density, the elastic moduli and their pressure derivatives, and the relative phase stability (between bcc and close packed). The axial stresses σ_i and elastic moduli C_{ij} are computed with the analytic formula derived in Ref. [9] [see Eqs. (A19), (A21), (A36), and (A37)]. To ensure *uniaxial* loading, and properly account for the Poisson effect, at each computational stage (i.e., for each value of longitudinal lattice parameter a_1), the transverse lattice parameters a_2 and a_3 are iterated to states where $\sigma_2 = \sigma_3 = 0$; on the orthorhombic paths, a_2 and a_3 are iterated independently.

Figure 1 illustrates the modes of uniaxial loading studied here; superscripts b and f are used to identify quantities reckoned specifically to the bc and fc axes, respectively. On the primary path, the crystal can be considered as either bct or fct; if the load "acts vertically" the bc cells in (a) and the fc cells in (b) are tetragonal on this path, as are the bold-lined fc and bc cells "to the left" in the figure. Crystal symmetry and the absence of transverse loads cause the appearance of three stress zeros on the primary path, i.e., where fct becomes fcc, where bct becomes bcc, and at a special unstressed tetragonal state [11]; these respective unstressed structures are designated F, B, and T; the lattice parameters in states F and B (on the primary path) are, respectively, $a_1 = a_2^f = a_3^f \equiv a^f$ and $a_1 = a_2^b = a_3^b \equiv a^b$. On both the primary and secondary paths, the axial stretches are $\lambda_1 = a_1/a^b$ and $\tilde{\lambda}_1 = a_1/a^f$, and the transverse stretches are $\lambda_i = a_i^b/a^b$ and $\tilde{\lambda}_i = a_i^f/a^f$ $(i = 2, 3)$. For a crystal in equilibrium with its environment, the incremental changes in axial loads δF_i following a δ departure from a given tetragonal state are $\delta F_1 = C_{11}^* \delta a_1 + C_{12}^*(\delta a_2 + \delta a_3)$, $\delta F_2 = C_{12}^* \delta a_1 + C_{22}^* \delta a_2 + C_{23}^* \delta a_3$, and $\delta F_3 = C_{12}^* \delta a_1 + C_{23}^* \delta a_2 + C_{22}^* \delta a_3$, where $C_{ij}^* \equiv \partial^2 E_{\text{bind}}/\partial a_i \partial a_j$, reckoned relative to either the bct or fct crystal axes. If the load remains uniaxial, $F_2 = F_3 = \delta F_2 = \delta F_3 = 0$, and a general solution is $\delta a_2 = \delta a_3 = [-C_{12}^*/(C_{22}^* + C_{23}^*)]\delta a_1$, with $\delta F_1/\delta a_1 = C_{11}^* - 2C_{12}^{*2}/(C_{22}^* + C_{23}^*)$, i.e., the primary path of tetragonal symmetry. However, if the primary path contains a "special invariant eigenstate" [7], where $C_{22}^* = C_{23}^*$ (or equivalently, $C_{22} = C_{23}$), the above equations admit bifurcation under dead load ($\delta F_1 = \delta F_2 = \delta F_3 = 0$) with $\delta a_1 = 0$, $\delta a_2 = -\delta a_3$, i.e., bifurcation from tetragonal to orthorhombic under strict uniaxial load. Also, the primary and secondary internal energy paths are of course tangent at the branch point.

In the present Letter, the primary path of each alkali metal exhibits two $C_{22} = C_{23}$ states, one on the bct axes (i.e., $C_{22}^b = C_{23}^b$) and the other on fct ($C_{22}^f = C_{23}^f$); crystal symmetry under uniaxial load causes $C_{44}^b = 0$ simultaneously with $C_{22}^f = C_{23}^f$, likewise for $C_{44}^f = 0$ and $C_{22}^b = C_{23}^b$. Figures 2 and 3 show the relevant C_{ij} and associated branching behavior of Rb as an example. The "left-hand branch" (lhb) point for each alkali metal occurs in compression at $C_{22}^b = C_{23}^b$ for values of λ_1 in the range 0.951 (for Cs) to 0.964 (for Li); the "right-hand branch" (rhb) originates in tension at $C_{22}^f = C_{23}^f$ with $\tilde{\lambda}_1$ ranging from 1.038 (for Cs) to 1.053 (for Li). Each of these branch points terminates stable ranges on the primary path.

The lhb and rhb exhibit an interesting one-to-one symmetrical correspondence. This is made evident from the following unified discussion, wherein the first entry of "double entry brackets $\{\ldots\backslash\ldots\}$" describes behavior on or leading to the lhb and the second ... the rhb. Consider a [100] uniaxial {compressive\tensile} load applied to the initially {bcc(B)\fcc(F)} crystal. The crystal first follows the primary path in the region $\{\lambda_1 \leq 1 \backslash \tilde{\lambda}_1 \geq 1\}$, with $\{\lambda_2^b = \lambda_3^b > 1 \backslash \tilde{\lambda}_2^f = \tilde{\lambda}_3^f < 1\}$; although both bct and fct describe the structure throughout this path, let us focus on the {bc\fc} structure illustrated in Fig. 1 {a\b}. At the $C_{22} = C_{23}$ eigenstate, branching from tetragonal to orthorhombic, under dead load, occurs with $\delta a_1 = 0$, $\{\delta a_2^b = -\delta a_3^b \backslash \delta a_2^f = -\delta a_3^f\}$; with complete generality, assume $\{\delta a_2^b < 0 \backslash \delta a_2^f > 0\}$. Following bifurcation, δa_2 would be expected to vary much faster than δa_1, since

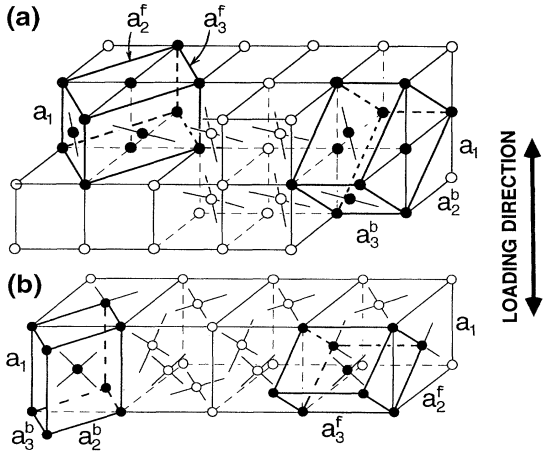

FIG. 1. Two ways of viewing the crystal under uniaxial load: (a) fc cells (bold lines) in a bc lattice structure, (b) bc cells (bold lines) in a fc lattice structure.

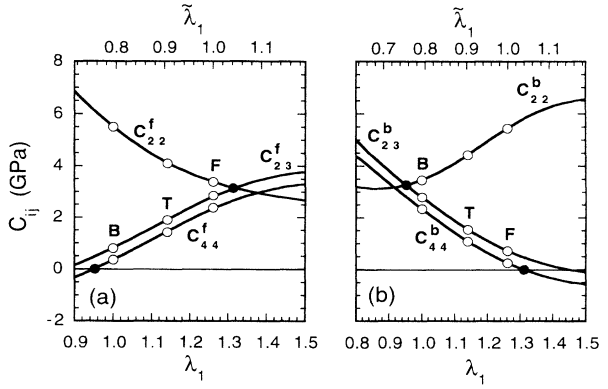

FIG. 2. Elastic moduli C_{ij} on the primary path versus axial stretch for Rb; the moduli are reckoned relative to (a) the fct axes and (b) the bct axes.

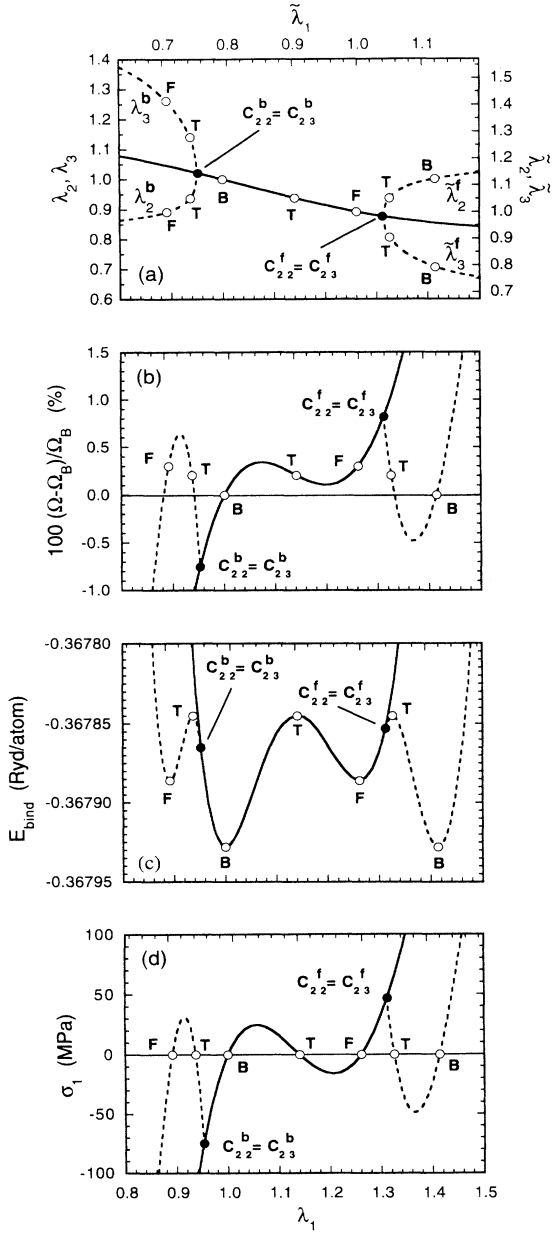

FIG. 3. Behavior on the primary tetragonal (—) and secondary orthorhombic branch (- - -) paths for Rb (the upper abscissa scale on each plot is $\tilde{\lambda}_1$ and the lower is λ_1): (a) transverse stretch, (b) variation in volume per atom Ω (Ω_B is Ω in state B), (c) internal energy, and (d) uniaxial stress.

$|\delta a_2/\delta a_1|$ is infinite at the bifurcation (on the branch path). Thus, while $a_1\{<a_2^b \backslash > a_2^f\}$ at the branch point, soon after branching a_1 and $\{a_2^b \backslash a_2^f\}$ become equal; when this happens, the bold-lined cell in the right-hand portion of Fig. 1 $\{a \backslash b\}$ becomes tetragonal, and the magnitude of the axial load must drop to zero (since the tetragonal symmetry implies $F_1 = F_2$, and F_2 is of course zero); these unstressed states are identical to the unstressed state T on the primary path, but differently oriented. In addition, since the nature of atomic forces causes the load to be {compressive\tensile} under {small\large} axial stretch, with still further {decrease\increase} of axial stretch, the load F_1 must pass through a second zero on the branch path; this occurs coincident with $a_1 = \{a_2^b = a_3^b/\sqrt{2} \backslash a_2^f = a_3^f\sqrt{2}\}$, i.e., where the bold-lined cell (to the right) in Fig. 1 $\{a \backslash b\}$ becomes {fcc\bcc} on the {lhb\rhb}; these states are identical to the cubic states $\{F \backslash B\}$ on the primary path, differently oriented. In particular, cubic state $\{F \backslash B\}$ on the {lhb\rhb} path is seen to be oriented with *its* [110] axis parallel to the loading direction, and thus this path is identical to that of [110] uniaxial loading of the {fcc\bcc} structure.

Three distinct equilibrium paths for bcc → fcc transitions in the alkali metals under uniaxial loading are therefore (i) the (simplest and most "well-known") Bain path (i.e., [100] uniaxial tension on the primary path), (ii) [100] uniaxial *compression* which takes the bcc structure into fcc via the bifurcation to the secondary lhb path at $C_{22}^b = C_{23}^b$, and (iii) [110] uniaxial compression of the bcc structure, wherein the initial equilibrium loading configuration is described by the rhb path, which branches to the primary path at $C_{22}^f = C_{23}^f$. (The analogous fcc → bcc transitions are just the reverse paths.) For a given alkali metal, the "energy barrier" (or maximum energy on the equilibrium transformation path) is identical for each of the bcc ⇄ fcc transitions; this maximum occurs at each state T. This is in accord with a recent hypothesis [12] that the minimum energy barrier for any homogeneous bcc ⇄ fcc transition, on an equilibrium path between unstressed and elastically stable initial and final states, is that associated with the unstressed tetragonal configuration that appears on the uniaxial loading Bain path. The stress barriers, however, are distinct on each path; e.g., for Rb, the theoretical stresses required to initiate the bcc → fcc transformation are 24.7 MPa in [100] tension, 74.8 MPa in [100] compression, and 48.9 MPa in [110] compression. This has interesting ramifications for Na or Li in their bcc configurations, at temperatures close to their bcc → close packed transitions. Our results suggest that the transitions could be induced by *either* [100] tension or compression, as well as [110] compression.

Some of the theoretical behaviors displayed in Fig. 3 depend mainly on crystal symmetry and the *general nature* of interatomic forces (i.e., repulsive and attractive at large and small distances, respectively), while others are sensitive to the *details* of atomic binding and hence are model dependent. For example, the general shape of the *primary* σ_1 curve (i.e., three stress zeros) is a result of crystal symmetry [11], whereas the *order of appearance* of the unstressed states B, T, and F on this curve is model dependent. (The possible existence of four stress zeros would be precluded by the physical conditions requiring the crystal to be under compression at very small λ_1 and in tension at very large λ_1; five zeros are possible, but unlikely.) The fcc

state will always reside "to the right" of the bcc state (λ_1 will always be greater in the fcc state than in the bcc state, owing to crystal symmetry). Thus, there are three possible orderings: (1) B, T, F (as found for the alkalis); (2) T, B, F; and (3) B, F, T. The centrally located unstressed state on the primary path is necessarily unstable, owing to the falling load characteristic, while either (or both) of the other unstressed states may be stable elastically, depending on the values of the elastic moduli in these states. Thus, systems that possess mechanically stable fcc and bcc structures (at zero stress) exhibit case (1) behavior. Cases (2) and (3) allow the existence of stable, unstressed, bct (or equivalently fct) structures, although case (3) has yet to be observed computationally. We have also completed analogous computations for pseudopotential and simplified pseudopotential models of the noble metals; this work will be the subject of a full length paper.

Briefly, the noble metals exhibit case (2) behavior (i.e., bcc is unstable); two eigenstates $C_{22} = C_{23}$ are also found on the primary path; the state $C_{22}^f = C_{23}^f$ terminates a stable region in tension (as in the alkalis) but the $C_{22}^b = C_{23}^b$ state is embedded in an unstable region of falling load characteristic on the primary path; the general behavior on the two secondary paths is similar to that of the alkalis, except the states B and T are interchanged on the rhb secondary path. The models employed in these computations are described in Ref. [13]. Suitable adjustment of the potential parameters can cause these systems to acquire case (1) behavior, wherein the results are very similar to those of the alkalis (i.e., both bcc and fcc are stable and both $C_{22} = C_{23}$ states terminate stable ranges on the primary paths, with the same characteristic secondary paths branching therefrom). This behavior is of particular interest because of its applicability to the stable bcc β-brasses (which also undergo various martensitic transformations).

In summary, the appearance of the $C_{22} = C_{23}$ states on the primary path, while evidently dependent on the specifics of atomic binding, seems fairly general; if such states do occur, the salient features of the secondary branch paths are then largely owed to crystal symmetry and the general nature of interatomic forces. The theoretical results suggest various infinitesimal strain phenomena that may be verified experimentally, including a negative Poisson ratio in [110] loading of bcc and fcc crystals (since the secondary path variations of λ_2 and λ_3 with λ_1 are of opposite sign), upward and downward concavities of the [110] and [100] bcc loading curves, respectively, and the opposite concavities of the respective fcc loading curves [the curvatures are evident in Fig. 3(d)]. The negative Poisson ratios have been verified from experimental elastic constant data and direct measurement [14,15]. The loading curvatures apparently have not yet been measured for the alkali metals, although the [100] and [110] loading curves of the bcc β-brasses fit the theoretical model [15] as do those of fcc crystals, in general [14].

Finally, we mention that many investigators (see, e.g., Refs. [16–19]) have computed binding energies on "classical" homogeneous bcc $\rightleftarrows$ fcc transformation (e.g., Bain, Zener, or Bogers-Burgers) paths that are defined by the monotonic variation of specific *strain* parameters. While there are some obvious similarities between such studies and ours, the present work stands in contradistinction, as here it is the *loading environment* that is well defined and controlled; without specification of the loads acting on the crystal, there can be no study of the bifurcation process (i.e., branching from a primary to a secondary transformation path, of lower energy and *different crystal symmetry, under the same mode of loading*). The path branchings, in turn, demonstrate the energetic equivalences and stress divergences on the three distinct bcc $\rightleftarrows$ fcc transformation paths, all of which occur under the same mode of loading, but under different crystal symmetry.

*Present address: NASA-AMES Research Center, Mail Stop 234-1, Moffett Field, CA 94035-1000.
†Present address: Sandia National Laboratories, MS 0820, P. O. Box 5800, Albuquerque, NM 87185-0820.

[1] E. Kaxiras and L. L. Boyer, Phys. Rev. B **50**, 1535 (1994).
[2] J. Wang, S. Yip, S. R. Phillpot, and D. Wolf, Phys. Rev. Lett. **71**, 4182 (1993).
[3] R. J. Gooding, Y. Y. Ye, C. T. Chan, K. M. Ho, and B. N. Harmon, Phys. Rev. B **43**, 13 626 (1991).
[4] D. A. Young, *Phase Diagrams of the Elements* (University of California Press, Berkeley, 1991).
[5] F. Milstein and K. Huang, Phys. Rev. B **18**, 2529 (1978).
[6] R. Hill, Math. Proc. Cambridge Philos. Soc. **77**, 225 (1975).
[7] R. Hill and F. Milstein, Phys. Rev. B **15**, 3087 (1977).
[8] F. Milstein and B. Farber, Phys. Rev. Lett. **44**, 277 (1980).
[9] D. J. Rasky and F. Milstein, Phys. Rev. B **33**, 2765 (1986).
[10] F. Milstein and D. J. Rasky (to be published).
[11] F. Milstein, Solid State Commun. **34**, 653 (1980).
[12] F. Milstein, H. E. Fang, and J. Marschall, Philos. Mag. A **70**, 621 (1994).
[13] F. Milstein and D. J. Rasky, Phys. Rev. B **33**, 2341 (1986).
[14] F. Milstein and D. J. Rasky, Philos. Mag. A **45**, 49 (1982).
[15] F. Milstein and J. Marschall, Philos. Mag. A **58**, 365 (1988).
[16] R. M. Wentzcovitch and H. Krakauer, Phys. Rev. B **42**, 4563 (1990).
[17] J. Rifkin, Philos. Mag. Lett. **49**, L31 (1984).
[18] T. Suzuki and H. M. Ledbetter, Philos. Mag. A **48**, 83 (1983).
[19] P. Beauchamp and J. P. Villain, J. Phys. (Paris) **44**, 1117 (1983).